TRANSACTIONS ON EMERGING TELECOMMUNICATIONS TECHNOLOGIES
Trans. Emerging Tel. Tech. (2016)
Published online in Wiley Online Library (wileyonlinelibrary.com). DOI: 10.1002/ett.3011

SPECIAL ISSUE PAPER

Throughput, energy and overhead of multicast device-to-device communications with network-coded cooperation

Néstor J. Hernández Marcano[1,2]*, Janus Heide[1], Daniel E. Lucani[2] and Frank H. P. Fitzek[2]

[1] Steinwurf ApS, Aalborg, Denmark
[2] Department of Electronic Systems, Aalborg University, Aalborg, Denmark

ABSTRACT

Cooperation strategies in mobile networks typically rely in short-range technologies, like LTE-A device-to-device communications, for data exchange between devices forming mobile clouds. These communications provide a better device experience because the clouds offload the network. Nevertheless, this assumes that the throughput gains and energy savings in multicasting are much larger between devices than the base station to the receivers. However, current mobile networks suffer from many different issues varying the performance in data rates, which calls into question these assumptions. Therefore, a first objective of this work is to assess the operating regions where employing cooperation results in higher throughput and/or energy savings. We consider multicast scenarios with network-coded mechanisms employing random linear network coding (RLNC). However, although RLNC is good for low amount of transmissions in multicast, it has an inherent overhead from extreme high or low field-related caveats. Thus, as a second objective, we review and propose the application of new network codes that posses low overhead for multicasting, by having a short representation and low dependence probability. We provide an analytical framework with numerical results showing (i) gains of several fold can be attained even if the in-device data rates are moderately larger (2×) than the cellular link data rate and (ii) that is feasible to attain less than 3% total mean overhead with the proposed codes. This is fairly lower than what can be achieved with RLNC schemes in most of the considered cases and achieving at least 1.5–2× gains. Copyright © 2016 John Wiley & Sons, Ltd.

***Correspondence**
N. J. Hernández Marcano, Steinwurf ApS, Aalborg, Denmark.
E-mail: nestor@steinwurf.com, nh@es.aau.dk

Received 5 July 2015; Revised 14 October 2015; Accepted 25 November 2015

1. INTRODUCTION

Data traffic is expected to grow by an order of magnitude for wireless mobile devices to support many data demanding services as shown in Figure 1 [1]. Common services of this type are video multicasting or local multimedia content sharing. From the perspective of the mobile users, high perceived quality and a low battery drain are important. For operators, their goal is to serve the highest number of users with the least amount of network resources and energy consumption from their infrastructure. In this scenario, both multicast and cooperation provide better performance than unicast, because several devices are served with the same communication resources.

Then, mechanisms that can offload network infrastructures have gathered significant interest from both academia and industry. Thus, there is a general interest from both academia [2, 3] and industry [4] in finding strategies that reduce mobile network usage by offloading the infrastructure to other types of short-range communications like device-to-device (D2D) or Wi-Fi. For this purpose, wireless cooperative *mobile clouds* [5, 6] are formed by receivers helping the cellular network by locally exchanging missing data packets instead of directly requesting them from it. Thus, cooperative techniques result in increased reliability, coverage extension and even increased throughput to end receivers. This potential has resulted in the inclusion of D2D communications in the 3rd Generation Partnership Project standardisation efforts. To recover from packet erasures in the wireless medium, typically rateless codes are employed as a forward error correction technique. Nevertheless, although they provide benefits for a broadcast scenario, they cannot be deployed for cooperative communications without affecting their

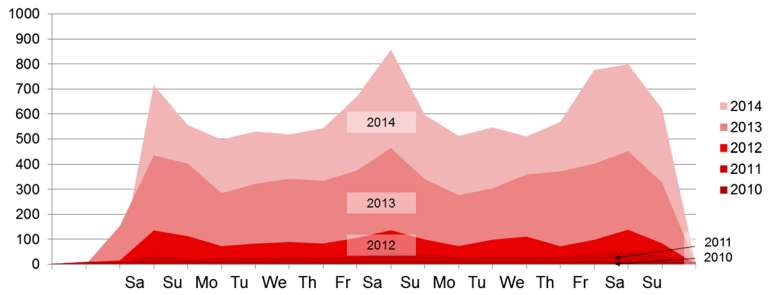

Figure 1. Average Oktoberfest data load for the 2010–2014 period (generic data units).

performance or decoding the data for each hop. Thus, there is a need for code schemes to overcome these drawbacks.

In this context, network coding [7], and particularly random linear network coding (RLNC) [8], not only provides a faster and more efficient approach to broadcast the data to the users, as shown by [9], but also simplifies the cooperation process because (i) the devices only need to know the number of linear combinations available and (ii) transmissions from a single device during the cooperation process can have a larger impact for the end receivers, given that a single transmissions can help different devices at the same time. This intuition has been exploited in previous works ranging from analysis to optimal policies and practical mechanisms, for example, Khamfroush *et al*. [10, 11].

However, the underlying assumption is that the cooperative channel is considerably faster than the channel to the base station and that energy costs are much lower because of proximity. Although this assumption was reasonable long ago, now the much higher data rates achievable in Long Term Evolution-Advanced (LTE-A) call this assumption into question. Also, if the devices cooperate using D2D of LTE-A, the data rate for cooperation will also be limited by the common channel and could be the same data rate in some cases. Thus, one goal of this paper is to review the problem of device cooperation focusing on the specific regions of operation where it can bring gains in throughput and energy.

Some of the analysis of mean performance for cooperative schemes has been carried out before, for example, Heide *et al.* [6, 12]; however, this paper provides a comprehensive study of the distributions of the number of transmitted packets for various scenarios. We define the natural concept of stable throughput for cooperative schemes. To the best of our knowledge, this has not been considered before because of the conventional assumption that the cellular data rate is the bottleneck in the communication process.

A second important factor that may affect the performance of the network is the coding scheme choice. The reason being that if a code does not employ resources properly, it reduces even more the benefits of throughput and energy in the short-range links. Here, RLNC considers creating linear combinations from a single network flow to distribute data between many devices. In order to reduce complexity and delay, transmissions of packet batches from the original data, called generations, were introduced in [13] as a technique to accomplish this. RLNC's flexibility to adapt to different network topologies makes it an interesting choice for upcoming networking protocols. Although, given that the random coefficients are picked from a single field, RLNC-based techniques have the caveat of introducing overhead due to mainly two reasons in the coding process. First, transmissions of linearly dependent (l.d.) packets occur due to the random selection of the coefficients [14, 15]. Second, in order to later perform decoding, typically the easiest goes for the coding coefficients to be appended to each coded packet before being sent through the network.

Different works have been made to observe the effects of RLNC parameters, for example, generation and field size [16], not only for the overhead but also for other metrics such as energy consumption and processing speed [17] among others. Variants of RLNC have been proposed to exploit a particular code structure to obtain a low overhead without compromising other metrics [18]. More recently, in [19], *telescopic codes* (TC) were introduced applying composite extension fields within a single generation, with the goal of reducing the total overhead while preserving recoding. Its parameters and performance were analysed for an ideal unicast scenario, but their potential for unreliable multicast scenarios was not explored.

In [20] and [21], the authors develop new optimised transmission and coding schemes based on RLNC for content distribution. However, they only consider broadcast and exclude cooperation. Also, these studies have a strong focus on video streaming, while in our case, we deal with distributing data in general. Furthermore, they do not consider the overhead of the code. In [22–25] can be found the advantages of employing multicast schemes with D2D capabilities. Although, these works do not consider both cooperation and network coding at the same time, making it difficult to evaluate the benefits of network coding in these scenarios. In this work, we pursue two goals: we (i) analyse the throughput and energy gains of network-coded cooperation and (ii) propose the employment of TC as a technique for minimising the overhead in heterogeneous, unreliable, cooperative networks. We provide a full analysis with a set of numerical results for both the region gains with RLNC and the use of TC for low overhead. We make this analysis for three scenarios in multicast sessions,

namely, broadcast, single cloud cooperation and multiple clouds cooperation for D2D communications, because they provide more benefits than others like unicast. Moreover, for the employment of TC, we compute the set of composite fields required to minimise the total overhead, which we define for broadcast and single cloud cooperation.

Our work is organised as follows: Section 2 introduces our system and general assumptions. Section 3 describes the code schemes and scenarios that we review indicating how the information is conveyed through the network. Analysis of the proposed coding schemes and transmission scenarios is made in Section 4. Later, Section 5 shows the considered metrics in our study with the numerical results provided in Section 6. Final conclusions are presented in Section 7. The proofs of the used lemmas and corollaries in our study are in the Appendix.

2. SYSTEM MODEL

We consider the problem of reliably transmitting a set of packets from a source to N receivers in a cellular network under various transmission scenarios. The set constitutes a generation of g packets, which we code using RLNC with field size q. We consider a general topology as shown in Figure 2 where receivers might form D2D-based mobile clouds with multicast capabilities. Devices that are relatively close together create fully interconnected clouds.

In general, we may have C clouds, where each cloud has N_n users with $n \in [1, C]$ and $N = \sum_{n=1}^{C} N_n$. Here, in each cloud, we differentiate two types of devices. First, we refer as *heads* the devices with both cellular connectivity to the source and all others in the cloud. Then, we have $H_n \leqslant N_n$ heads per cloud. Second, the *non-heads* are the devices without a cellular connection but only to all others, for example, $N_n - H_n$ non-heads per cloud. For our study, we briefly observe the dominating regimes for heterogeneous cloud sizes to notice that the homogeneous cloud size provides the best performance in terms of total transmission time. Therefore, we review the case of having a homogeneous cloud size, for example, the same number of users in each cloud $N_n = N_{uc}\ \forall\ n$, giving $N = C \times N_{uc}$, because this is the ideal operational regime.

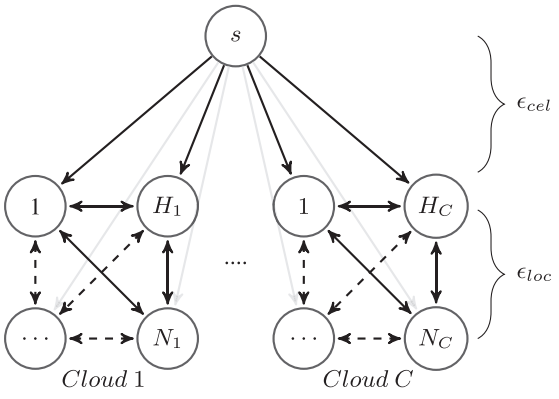

Figure 2. Topology of C device-to-device mobile clouds.

We consider independent packet erasure rates on the connectivity links from the source to the heads, ϵ_{jn}, $j \in [1, H_n]$, $n \in [1, C]$; for example, the packet reception distribution of receiver j is $Bernoulli(1-\epsilon_{jn})$ and is independent from all others. We will provide the general expressions for scenario distributions with heterogeneous cellular links, but for evaluation purposes, we will consider all these erasures equal to ϵ_{cel}. Similarly, inside any cloud, all the connections can be regarded as bidirectional symmetric channels via D2D. These links have homogeneous, independent and identically distributed erasure rates, which we consider equal to ϵ_{loc} for simplicity.

To guarantee interference management and proper content delivery, we assume an underlay D2D mobile network. In this way, we review the transmission scenarios once a previous and arbitrary cellular network resource allocator has assigned the communications resources in it. Once network management has been addressed, packets are either sent under a broadcast ($N_{uc} = 1$), multiple cloud ($1 < N_{uc} < N$) or single cloud ($N_{uc} = N$) cooperation transmission scenarios.

Thus, in any scenario, for convenience, we consider that $C + 1$ physical communication resources have already been allocated. Nevertheless, if $K < C + 1$ are only available, standard cellular techniques such as frequency reuse patterns can be employed. Then, two clouds using the same frequency will be geographically separated long enough to ensure the reuse of communication resources without causing interference. We consider this to perform the transmissions between the source and all the clouds through *multicast groups*. First, a multicast group is created between the source and all cloud heads to transmit the content to each cloud collectively. Second, C multicast groups are created between the heads of each of the C clouds and their respective non-heads, to cover missing packets. In this stage, the network controller is in charge of the coordination regarding on how the nodes must share their content into its own cloud.

Inter-cloud interference is defined as the reception of a transmission from a cloud where a receiver does not belong, which occurs when a transmission of that receivers cloud has been made during the same time slot. The interference generates a reduction in the signal-to-interference-plus-noise ratio, which increases the erasure rate and degrades the reception, possibly forcing retransmissions. Hence, we assume that cloud transmissions take place in orthogonal resources to ensure that inter-cloud interference does not occur. In case there are no available resources, techniques such as frequency reuse planning from mobile networks help to avoid this interference. For example, two clouds using the same frequency will be geographically separated enough to ensure there is no interference, making possible to reuse communications resources.

We consider the scenario where an acknowledgment (ACK) is sent only in two cases: first, when a receiver has collected g linearly independent (l.i.) coded packets and

second, for the cooperative case, when a cloud has g l.i. coded packets as a group. The ACK is sent through a reliable communications channel. Thus, only one ACK per generation of packets per receiver is sent. This makes a total of N feedback packets, differing from the case where ACKs are sent on a per-packet and per-receiver basis, which would result in $g \times N$ feedback packets. In other words, this reduces the feedback transmissions by a factor of g. If feedback is not wanted (or possible), a fixed number of extra transmissions can be sent ensuring some target reliability level, for example, 99%. However, because the number of transmissions is fixed, such an approach will lead to an additional transmission overhead particularly if the channel is time varying.

3. CODING SCHEMES AND TRANSMISSION SCENARIOS

In this section, we first consider and describe two coding schemes. Afterwards, we describe the three transmission scenarios considered in our study, namely, broadcast, single cloud cooperation and multiple clouds cooperation. We review them going from the simplest to the most elaborated scenario. Regarding the coding schemes, first, in all the scenarios, the source or the heads employ RLNC as a coding scheme. Second, for only broadcast and single cloud cooperation, we employ TC [19]. These types of codes possess very low overhead. The reason is that they are tailored for a given network to provide the best trade-off between both the overhead caused by (i) transmissions of l.d. packets and (ii) sending the coding coefficients for any receiver to be able to decode.

To accomplish this, TC relies on *composite extension finite fields*. This type of fields enables an encoder to create coded packets in an RLNC fashion but with some differences. The key idea for TC with composite fields is the following: Instead of picking all coding coefficients from a single field q inside a generation of size g, the encoder selects each coding coefficient $\boldsymbol{v}_j$, $j \in [1, g]$ in the generation from $GF(\boldsymbol{q}_j)$. Here, $\boldsymbol{q}$ is a vector that contains all the field sizes employed for each of the coding coefficients. Each of the field sizes follows a specific pattern. The chosen pattern makes compatible finite fields arithmetics from different fields in the same generation. In the subsequent sections, we give a brief description of RLNC because it is well known in the network coding literature. However, we provide further details for TC because they were recently introduced. Also, as we will see in our framework, RLNC will be regarded as a special case of TC that occurs when $\boldsymbol{q}_i = q \ \forall i \in [1, g]$. Thus, we will focus the following section on describing TC and its operations.

3.1. Coding schemes

3.1.1. Random linear network coding.

For this conventional coding scheme, we may create an encoded packet, create a recoded packet from a previous set or decode any set g coded packets performing Gaussian elimination on the $g \times g$ coding matrix. In general, we consider a field size q from which we take the coding coefficients and perform predefined Galois Field (GF) arithmetics. As follows, we will see that this is a special case of TC.

3.1.2. Telescopic codes.

We consider coding g packets, $\boldsymbol{m}_j, j \in [1, g]$ in the generation, each of size B bits. We define $\boldsymbol{q}$ as a vector containing each of the field sizes $\boldsymbol{q}_j$, we assume $\boldsymbol{q}_j \leqslant \boldsymbol{q}_{j+1}, \forall j \in [1, g]$ without loss of generality. Then, coded packets are generated in a similar fashion as with RLNC. However, each coding coefficient in an encoding vector $\boldsymbol{v}$ is chosen uniformly at random from a finite field $GF(\boldsymbol{q}_j), j \in [1, g]$ differing from RLNC. To keep valid field arithmetics, TC are based on composite extension finite fields of the form $\mathbb{F}_{2^k}$ with $k \in [1, 2, 4, 8, \ldots]$ in general. The key idea in composite extension fields is to design the arithmetic operations of a new extended finite field from the operations of a base field. With the extended field, we can continue the process and create another extension and so on. These fields are designed to allow compatibility for the operations performed among them. The composite fields are defined and described in [19]. Nevertheless, we give a brief overview of its operations to have a description for our analysis in Section 4.

3.1.3. Encoding.

A generic coded packet, $\boldsymbol{c}_i$, is generated by an encoder by mixing linear combinations of g packets. Here, packet $\boldsymbol{m}_j$ is regarded as an element from $GF(\boldsymbol{q}_j)$ and is multiplied by a coding coefficient $\boldsymbol{v}_{i,j}$ chosen uniformly at random from $GF(\boldsymbol{q}_j)$. Thus, a resulting coded packet of size B and its coding can be expressed as:

$$\boldsymbol{c}_i = \bigoplus_{j=1}^{g} \boldsymbol{v}_{i,j} \otimes \boldsymbol{m}_j \tag{1}$$

$$|\boldsymbol{v}_i| = \sum_{j=1}^{g} |\boldsymbol{v}_{i,j}| = \sum_{j=1}^{g} \lceil \log_2(\boldsymbol{q}_j) \rceil \text{ [bits]} \tag{2}$$

3.1.4. Decoding.

To perform decoding, we define $\boldsymbol{c} = \left[\boldsymbol{c}_1 \ldots \boldsymbol{c}_g\right]^T$ and $\boldsymbol{m} = \left[\boldsymbol{m}_1 \ldots \boldsymbol{m}_g\right]^T$. Decoding reduces to solve the linear system $\boldsymbol{c} = \boldsymbol{V} \cdot \boldsymbol{m}$ using Gaussian elimination [26]. Here, the coding matrix $\boldsymbol{V}$ contains any set of g l.i. packets $\boldsymbol{c}_i$ as rows as follows:

$$\boldsymbol{V} = \begin{bmatrix} \boldsymbol{v}_1 \\ \hline \vdots \\ \hline \boldsymbol{v}_g \end{bmatrix} = \begin{bmatrix} \boldsymbol{v}_{1,1} & \ldots & \boldsymbol{v}_{1,g} \\ \vdots & \ddots & \vdots \\ \boldsymbol{v}_{g,1} & \ldots & \boldsymbol{v}_{g,g} \end{bmatrix} \tag{3}$$

The decoder begins removing the contributions of the smallest field pivot elements , for example, leftmost elements in the main diagonal of (3). Once that information

DOI: 10.1002/ett

is known to the decoder, it proceeds in the same way for the next upper field in the composition using operations of the current field and so on to obtain the original set of packets [19].

3.1.5. Recoding.

Given the picking of elements from different fields, recoding needs to be properly defined to ensure that the coefficients of a recoded packet cannot be differentiated from a single coded one. Different approaches are described in [19]. For the scope of this study, we considered recoding in the lowest available field in the generation because it preserves recoding with low overhead in the encoding vector. Nevertheless, the major problem in this approach is the increase of more l.d. packets for the last transmissions in a given generation. In this way, let us define a generic recoded packet as $\tilde{\boldsymbol{c}}_i$ and its corresponding encoding vector as $\tilde{\boldsymbol{v}}_i$ as follows:

$$\tilde{\boldsymbol{c}}_i = \bigoplus_{j=1}^{g} \boldsymbol{w}_{i,j} \otimes \boldsymbol{c}_j \tag{4}$$

$$\tilde{\boldsymbol{v}}_i = \bigoplus_{j=1}^{g} \boldsymbol{w}_{i,j} \otimes \boldsymbol{v}_j \tag{5}$$

In (4) and (5), $\boldsymbol{w}_{i,j}$ is the coding coefficient that multiplies $\boldsymbol{c}_j$, uniformly and randomly chosen from $\min(\boldsymbol{q})$. Any decoder that collects $\tilde{\boldsymbol{c}}_i, i \in [1, g]$ l.i. packets, with their $\tilde{\boldsymbol{v}}_i$, will be able to decode the whole generation as described in Section 3.1.4.

3.2. Transmission scenarios

3.2.1. Broadcast.

For broadcast, $N_{uc} = 1$, the source generates an encoded packet and later attaches the coding coefficients values and sends it to all receivers through the erasure channels described in Section 2. When a packet successfully arrives at a receiver, it checks if the packet is l.i. from all its previous. If not, it discards it. In case of being l.i., the receivers add it to its coding matrix. This process is repeated until all receivers have collected their required combinations. An ACK is sent through the feedback channel from the last receiver after it obtains its final combination. In this scheme, recoding is not used.

3.2.2. Single cloud cooperation.

In a single cloud cooperation scenario, $N_{uc} = N$ and packet transmissions take place in two stages. First, the source broadcasts coded packets to the heads through the cellular network, that is, the cellular stage, and second, internally between receivers, which have missing packets, in a network-coordinated fashion, that is, the local stage. For the cellular stage, the source broadcast coded packets for the cloud heads, because it is enough to obtain coded packets collectively to later recode them. Once the cellular stage has ended, for example, the g l.i. packets are in the cloud, there will be receivers that do not exactly have this quantity of packets to decode. To manage this, in the local stage, each head broadcasts recoded packets in a coordinated way to ensure all receivers obtain their remaining packets. For the case of TC, recoding will be performed in the lowest field. This stage finishes once all receivers have decoded the generation and any device in the cloud sends and an ACK through the feedback channel to the sender.

3.2.3. Multiple clouds cooperation.

For a cloud cooperation scenario, $1 < N_{uc} < N$, packet transmissions go in a similar way as before. However, two main differences exist. First, in the cellular stage, packets are broadcasted to the heads multicast group, instead of all in a single cloud. Hence, we use one multicast channel. Second, in the local stage, the C set of heads broadcasts recoded packets to all the other users inside their respective multicast groups. Again, this performed in a network-coordinated way to ensure all receivers obtain their remaining packets. This stage finishes once all receivers in all clouds have g l.i. coded packets and an ACK through the feedback channel to the sender.

4. SCENARIOS ANALYSIS

We proceed to study the underlying probability distributions for the number of transmissions required to decode either RLNC or TC within their respective transmission scenarios. With the statistical description of the transmissions, we perform two types of studies. First, we identify the regions where cooperation performs better than broadcast in terms of throughput and energy when RLNC is used. Second, for TC, we perform an overhead analysis for the transmission scenarios and evaluate them for three schemes that can be used with TC.

For the code and each transmission scenario, we model the number of transmissions to decode as a random variable to derive its probability mass function (pmf). We perform this in order to obtain reasonable approximations of the linear independence, erasure and transmission processes and also to separate the effect of the code from the scenario. We first give an expression of the pmf for RLNC, later we incorporate erasures in the process and finally compute the pmf for the transmission scenarios.

4.1. Coding scheme distributions

To calculate the distribution and pmf for either an RLNC or TC scheme in a generic fashion, we derive a framework for the pmf of TC distribution, and we will make the proper evaluations to differentiate with RLNC.

We first consider a single source-destination link without erasures. The process for obtaining each new l.i. packet can be modelled by the Markov Chain in Figure 3. This chain comprises $g + 1$ states. First, state i with $i \in [1, g]$ is the case where the i-th l.i. coded packet has not been received

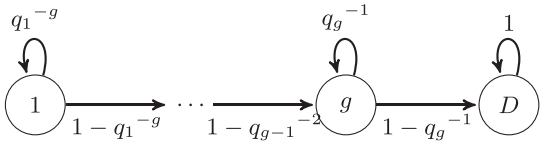

Figure 3. Absorbing Markov Chain for telescopic codes.

by the destination. Then, D is the absorbing state where decoding is performed.

The transition probabilities of each state depend not only on the amount of previously received l.i. combinations but also on the field chosen to represent the i-th coding coefficient. The model in Figure 3 is a reasonable approximation as described in [19] because, in the decoding process, non-received pivots from the lowest fields dominate the transition probabilities and tend to appear first.

We use a probability-generating function (pgf) approach with the key idea that each stage of the Markov Chain of TC in Figure 3 can be modelled as a geometric distribution and then compute the pmf from operations in the more tractable pgf domain.

Lemma 4.1 (*Telescopic codes probability mass function*)**.** *Consider the case of a single source-destination link without erasures that employs TC of generation size g field size* $\boldsymbol{q}$*. Let* $\mathbb{T}_{TC}$ *be the random number of transmissions required to decode. Then, the pmf of* $\mathbb{T}_{TC}$ *for the probability of decoding in exactly t transmissions is*

$$f_{\mathbb{T}_{TC}}(t;g,\boldsymbol{q}) = \Pr[\mathbb{T}_{TC}=t] = P_g \sum_{l=1}^{L}\sum_{n=1}^{m_l} a_{l,n}\binom{t-g+n-1}{t-g}{\gamma_l}^{t-g},\ t\in[g,\infty) \tag{6}$$

where in (6), $P_g = \Pr[\mathbb{T}_{TC}=g]$ *is the probability of decoding in exactly g transmissions,* $\binom{n}{k}$ *is the binomial coefficient defined as* $\frac{n!}{k!(n-k)!}$ *with* $n \geq k$ *and* $\gamma_l,\ l \in [1,L]$ *is one of the L distinct probabilities from the Markov Chain, which is repeated* m_l *times in the resulting Markov Chain. The* $a_{l,n},\ l\in[1,L],\ n\in[1,m_l]$ *are the residues of the pgf of (6) given by*

$$a_{l,n} = \frac{\lim_{z\to\gamma_l} \frac{d^{m_l-n}}{d(z^{-1})^{m_l-n}}\left(\frac{G_{\mathbb{T}_{TC}}(z^{-1})(1-\gamma_l z^{-1})^{m_l}}{P_g z^{-g}}\right)}{(m_l-n)!(-\gamma_l)^{m_l-n}} \tag{7}$$

Proof. The proof is in the Appendix. □

Corollary 4.1.1 (*RLNC* Distribution)**.** *The distribution and pmf for RLNC is given by*

$$f_{\mathbb{T}_{RLNC}}(t;g,q) = \Pr[\mathbb{T}_{RLNC}=t] = P_g\sum_{i=1}^{g} a_i{\gamma_i}^{t-g},\ t\in[g,\infty) \tag{8}$$

where in (8), the a_i *are given as follows:*

$$a_i = \prod_{m=1,m\neq i}^{g}\frac{1}{1-q^{m-i}} \tag{9}$$

Proof. The proof is in the Appendix. □

We include the analysis for a generic erasure ϵ by following a procedure, as made in [27], that considers all the disjoint cases by the law of total probability, where i l.i. coded packets where received in t transmissions and $t-i$ coded packets were received and l.i. The successful receptions are accounted by the negative binomial distribution[†] and the linear independence by (6). Then, the pmf for a unicast session with TC and erasures, $\mathbb{T}_U$, can be expressed as follows:

$$f_{\mathbb{T}_U}(t;g,\boldsymbol{q},\epsilon) = \Pr[\mathbb{T}_U=t] = \sum_{i=g}^{t}\binom{t-1}{i-1}(1-\epsilon)^i\epsilon^{t-i}f_{\mathbb{T}_{TC}}(i;g,\boldsymbol{q}),\ t\in[g,\infty) \tag{10}$$

4.2. Broadcast distribution

For broadcast, we can regard its pmf as the case of finding the required transmissions for the maximum of N independent parallel unicast sessions. This results in an upper bound because we exclude other policies that take advantage of common coded packets. Because each receiver just needs to collect different linear combinations to decode the packets, the number of transmissions will be bounded by the receiver that performs the worst. In this way, the number of transmissions for broadcast is given by $\mathbb{T}_B = \max_{j=[1,N]}\mathbb{T}_{U_j}$, where $\mathbb{T}_{U_j}$ is the distribution on which pmf is obtained from (10). We review this and prove it in the following lemma.

Lemma 4.2 (*Broadcast TC probability mass function*)**.** *Consider the case of a broadcast scenario with heterogeneous packet erasure rates* $\epsilon_j,\ j\in[1,N]$ *that employs TC of generation size g and field sizes* $\boldsymbol{q}$*. Let* $\mathbb{T}_B$ *be the random number of transmissions required to decode. Then, the pmf of* $\mathbb{T}_B$ *for the probability of decoding in exactly t transmissions is*

[†]We use the definition of the negative binomial distribution that accounts for the random number $\mathbb{T}$ of Bernoulli trials of success probability p required to attain n successes. Then, $\mathbb{T}\sim NB(n,p) \implies \Pr[\mathbb{T}=t] = \binom{t-1}{n-1}p^n(1-p)^{t-n},\ t\in[n,\infty)$.

$$f_{\mathbb{T}_B}(t;N,g,\boldsymbol{q},\epsilon_1,\ldots,\epsilon_N) = \prod_{j=1}^{N}\left(\sum_{k=g}^{t}\sum_{i=g}^{k}\binom{k-1}{i-1}(1-\epsilon_j)^i\epsilon_j^{k-i}f_{\mathbb{T}_{TC}}(i;g,\boldsymbol{q})\right) - \prod_{j=1}^{N}\left(\sum_{k=g}^{t-1}\sum_{i=g}^{k}\binom{k-1}{i-1}(1-\epsilon_j)^i\epsilon_j^{k-i}f_{\mathbb{T}_{TC}}(i;g,\boldsymbol{q})\right), \; t\in[g,\infty) \tag{11}$$

where in (11), $f_{\mathbb{T}_{TC}}(t;g,\boldsymbol{q})$ is the TC pmf given by (6).

Proof. The proof is in the Appendix. □

Corollary 4.2.1 (*Homogeneous erasures in broadcast*)**.** *The pmf of broadcast TC with homogeneous erasure rates, $\epsilon_1,\ldots,\epsilon_N=\epsilon$, is*

$$f_{\mathbb{T}_B}(t;N,g,\boldsymbol{q},\epsilon) = \left(\sum_{k=g}^{t}\sum_{i=g}^{k}\binom{k-1}{i-1}(1-\epsilon)^i\epsilon^{k-i}f_{\mathbb{T}_{TC}}(i;g,\boldsymbol{q})\right)^N - \left(\sum_{k=g}^{t-1}\sum_{i=g}^{k}\binom{k-1}{i-1}(1-\epsilon)^i\epsilon^{k-i}f_{\mathbb{T}_{TC}}(i;g,\boldsymbol{q})\right)^N, \; t\in[g,\infty) \tag{12}$$

Proof. It can be easily verified that evaluating (11) with homogeneous erasure rates, $\epsilon_j=\epsilon \;\forall j$, and doing the corresponding algebra, one obtains (12). □

4.3. Single cloud cooperation distribution

For single cloud cooperation, we consider its random number of transmissions for decoding, $\mathbb{T}_{SCC}$, as the sum of two random number of transmissions. First, we consider the random number of transmissions for the cloud to obtain g l.i. coded packets in the cellular stage, $\mathbb{T}_{SCC,cel}$. Second, we add the number of transmissions in the local stage required for all the devices to share their content, $\mathbb{T}_{SCC,loc}$, which is a particular case of broadcast under the proper evaluation. Hence, $\mathbb{T}_{SCC}=\mathbb{T}_{SCC,cel}+\mathbb{T}_{SCC,loc}$. We give a formal definition of this distribution and its proof in the following lemma.

Lemma 4.3 (*Single cloud cooperation TC distribution*)**.** *Consider the case of a single cloud cooperation scenario that employs TC of generation size g and field sizes $\boldsymbol{q}$. The cloud is composed of H heads from N devices with $H\leqslant N$. The heads have heterogeneous packet erasure rates ϵ_j , $j\in[1,H]$ for the links between the source and them. All devices inside the cloud have a homogeneous packet erasure rate ϵ_{loc} for all their $\frac{N(N-1)}{2}$ connection links between them. Then, the distribution for the random number of transmissions required for decoding is given by $\mathbb{T}_{SCC}=\mathbb{T}_{SCC,cel}+\mathbb{T}_{SCC,loc}$ where each term is given as follows:*

$$\mathbb{T}_{SCC,cel} = \mathbb{T}_U\left(g,\boldsymbol{q},\prod_{j=1}^{H}\epsilon_j\right) \tag{13}$$

$$\mathbb{T}_{SCC,loc} = \begin{cases}\mathbb{T}_B(N-H,g,\boldsymbol{q},\epsilon_{loc}), & H<N\\ \mathbb{T}_B(N_{loc},g_{loc},\boldsymbol{q},\epsilon_{loc}), & H=N\end{cases} \tag{14}$$

$$N_{loc} = N-\left\lfloor P_g\sum_{j=1}^{N}(1-\epsilon_j)^g\right\rfloor \tag{15}$$

$$g_{loc} = \max_{j\in[1,N]}\left(g-\left\lfloor(1-\epsilon_j)\sum_{i=1}^{g}p_i\right\rfloor\right) \tag{16}$$

where in (13) and (14) the parenthesis notation indicates the evaluation of the respective distribution with the given parameters. In (15) and (16), P_g and p_i are respectively the probabilities of linear independence at g transmissions and in each stage of the TC Markov Chain. Both are defined in the proof of Lemma 4.1.

Proof. The proof is in the Appendix. □

Corollary 4.3.1 (*Homogeneous conditions in single cloud cooperation*)**.** *The distribution of single cloud cooperation TC with homogeneous erasure rates, $\epsilon_1,\ldots,\epsilon_H=\epsilon_{cel}$, is*

$$\mathbb{T}_{SCC,cel} = \mathbb{T}_U\left(g,\boldsymbol{q},\epsilon_{cel}^H\right) \tag{17}$$

$$\mathbb{T}_{SCC,loc} = \begin{cases}\mathbb{T}_B(N-H,\boldsymbol{q},\epsilon_{loc}), & H<N\\ \mathbb{T}_B(N_{loc},g_{loc},\boldsymbol{q},\epsilon_{loc}), & H=N\end{cases} \tag{18}$$

$$N_{loc} = N-\left\lfloor P_gN(1-\epsilon_{cel})^g\right\rfloor \tag{19}$$

$$g_{loc} = g-\left\lfloor(1-\epsilon_{cel})\sum_{i=1}^{g}p_i\right\rfloor \tag{20}$$

Proof. By evaluating Equations 13–(16) with $\epsilon_j=\epsilon_{cel}\;\forall j$ □

4.4. Multiple clouds cooperation distribution

For multiple clouds cooperation, we consider its random number of transmissions for decoding, $\mathbb{T}_{MCC}$, again as the sum of two random number of transmissions in a cellular and local fashion as before. Hence, $\mathbb{T}_{MCC}=\mathbb{T}_{MCC,cel}+\mathbb{T}_{MCC,loc}$. However, in this scenario, for the local stage, consider the behaviour of the average user. We first derive the distribution for all the cloud and then evaluate for the average user. We give a formal definition of this distribution and its proof in the following lemma.

Lemma 4.4 (*Multiple clouds cooperation RLNC distribution*)**.** *Consider the case of a multiple clouds cooperation scenario that employs RLNC of generation size g and field*

size q. Each cloud is composed of H_n heads from N_{uc} devices with $H_n \leqslant N_{uc}$. The heads have heterogeneous packet erasure rates ϵ_{jn} , $j \in [1, H_n]$, $n \in [1, C]$ for the links between the source and them. All devices inside each of the C clouds have a homogeneous packet erasure rate ϵ_{loc} for all their $\frac{N(N-1)}{2}$ connection links between them. Then, the distribution for the random number of transmissions required for decoding each cloud is given by $\mathbb{T}_{MCC} = \mathbb{T}_{MCC,cel} + \mathbb{T}_{MCC,loc}$ where each term is given as follows:

$$\mathbb{T}_{MCC,cel} = \max_{n\in[1,C]} \left(\mathbb{T}_U \left(g, q, \prod_{j=1}^{H_n} \epsilon_{jn} \right) \right) \tag{21}$$

$$\mathbb{T}_{MCC,loc} = \begin{cases} \mathbb{T}_B(N_{uc} - H_n, g, q, \epsilon_{loc}), H_n < N_{uc} \\ \mathbb{T}_B(N_{uc,loc,n}, g_{loc,n}, q, \epsilon_{loc}), H_n = N_{uc} \end{cases} \tag{22}$$

$$N_{uc,loc,n} = N_{uc} - \left\lfloor P_g \sum_{j=1}^{N_{uc}} (1 - \epsilon_{jn})^g \right\rfloor \tag{23}$$

$$g_{loc,n} = \max_{j\in[1,N_{uc}]} \left(g - \left\lfloor (1 - \epsilon_{jn}) \sum_{i=1}^{g} p_i \right\rfloor \right) \tag{24}$$

Where in (21) and (22), the parenthesis notation indicates the evaluation of the respective distribution with the given parameters. In (23) and (24), P_g and p_i are respectively the probabilities of linear independence at g transmissions and in each stage of the RLNC Markov Chain. Both are defined in the proof of Lemma 4.1. Also important in the local stage, the number of transmissions depends on the n-th cloud being considered.

Proof. The proof is in the Appendix. □

With the previous distributions, we simply find a proper operation to observe the behaviour of the system. In our case, we consider the average cloud. To find the trends of the system, we simply evaluate the previous distributions in the homogeneous regime, for example, $\epsilon_{jn} = \epsilon_{cel}$, $\forall j, n$ and $H_n = H_c$, $\forall n$, which makes the average cloud equal to any cloud.

Corollary 4.4.1 (*Homogeneous conditions in multiple clouds cooperation*)**.** *The distribution of multiple clouds cooperation RLNC with homogeneous erasure rates, $\epsilon_{jn} = \epsilon_{cel}$, $\forall j, n$ and $H_n = H_c$, $\forall n$, is the following:*

$$\mathbb{T}_{MCC,cel} = \mathbb{T}_B \left(CH_c, g, q, \epsilon_{cel}^{H_c} \right) \tag{25}$$

$$\mathbb{T}_{MCC,loc} = \begin{cases} \mathbb{T}_B(N_{uc} - H_c, g, q, \epsilon_{loc}), \ H_c < N_{uc} \\ \mathbb{T}_B(N_{uc,loc}, g_{loc}, q, \epsilon_{loc}) \ , \ H_c = N_{uc} \end{cases} \tag{26}$$

$$N_{uc,loc} = N_{uc} - \lfloor P_g N_{uc} (1 - \epsilon_{cel})^g \rfloor \tag{27}$$

$$g_{loc} = g - \left\lfloor (1 - \epsilon_{cel}) \sum_{i=1}^{g} p_i \right\rfloor \tag{28}$$

Proof. The proof is performed by performing the mentioned evaluations in Equations 21–(24). Moreover, we notice that for the cellular stage, all erasure rates are the same, and the distribution for this stage reduces to employing a similar reasoning as the one in Corollary 4.2.1. □

5. PERFORMANCE METRICS

With the pmf for each scenario in Section 4, we compute the mean for the number of transmissions, which allows us to compute the throughput and energy. In the cloud cooperation scenarios, the results are relatively equivalent; however, the pmf in both cellular and local stages will depend on the scenario employed as shown in the previous section. Given this, for notation purposes, we omit the difference between $\mathbb{T}_{cel}$ and $\mathbb{T}_{loc}$ in single cloud cooperation and multiple clouds cooperation unless it is a necessary exception.

5.1. Throughput

We define the throughput in the cloud cooperation scenario for a given set of parameters in the following way:

$$R_{CC} = \frac{g}{\max(t_{cel} E[\mathbb{T}_{cel}], t_{loc} E[\mathbb{T}_{loc}])} \tag{29}$$

In (29), t_{cel} and t_{loc} are the durations of a time slot in the cellular and local stages, respectively. The effective rate perceived by a user will be the information sent divided by the completion time multiplied by a cost. For broadcast RLNC, the throughput is $R_B = \frac{g}{t_{cel} E[\mathbb{T}_B]}$.

5.2. Energy consumption

From the energy point of view, we only consider how much energy is required to transmit and receive a packet due to channel erasures. We do not consider the computational energy consumption because they are up to one order of magnitude below the energy expenditure for transmitting and receiving packets for moderate generation (up to 128) and field sizes (up to 2^8) [17], which we employ in our study. We consider that the energy for being idle is the same as for receiving a packet, because we have also observed that they are very close in practice [17].

To compute the energy consumption, we assume that a packet transmission and a packet reception spend the same energy because we observed this for commercial mobile devices in [17]. Then, we consider that the energy cost depends only on the type of connection employed. Therefore, we have two energy costs: E_{cel} for the cellular interface, and E_{loc} for the local interface. Each cost depends on the packet size and the energy per byte. The latter is proportional to the energy per bit for each type of connection. Then, naming the packet size p_s, the energy per byte E_B and the energy per bit E_b for the cellular stage,

we obtain $E_{cel} = p_s E_{B,cel}$ with $E_{B,cel} = 8E_{b,cel}$. Similarly, for the local stage, we obtain $E_{loc} = p_s E_{B,loc}$ with $E_{B,loc} = 8E_{b,loc}$. The energy per bit values are extracted from [28].

For our study, we compute the energy spent for the BS and the average energy spent per device for each transmission scenario. In the following, E_x indicates an energy value, and $E[]$ is the expected value operator for random variables. The energy expenditure for the BS, E_{BS}, is total number of cellular transmissions necessary before the heads in each cloud can decode the content jointly, multiplied by the energy cost of transmitting a packet on the cellular link. The average energy spent by a device, E_D, is computed from the following: (i) the reception of the heads in the cellular stage; (ii) the transmission of the heads in the local stage; and (iii) the reception of the non-heads in the local stage. The average is computed by dividing the previous total energy by the number of devices.

First, the energy consumption for broadcast is as follows:

$$E_{BS} = E_{cel} E[\mathbb{T}_B] \, , E_D = E_{cel} E[\mathbb{T}_B] \tag{30}$$

Second, the energy expenditure for the single cooperation scenario is shown in (31).

$$\begin{aligned} E_{BS} &= E_{cel} E[\mathbb{T}_{cel}] \\ E_D &= E_{cel} \left(\frac{H}{N} \right) E[\mathbb{T}_{cel}] + E_{loc} E[\mathbb{T}_{loc}] \end{aligned} \tag{31}$$

For the multiple clouds cooperation scenario, the result is equivalent with the number of heads and users per cloud equal to H_c and N_{uc}:

$$\begin{aligned} E_{BS} &= E_{cel} E[\mathbb{T}_{cel}] \\ E_D &= E_{cel} \left(\frac{H_c}{N_{uc}} \right) E[\mathbb{T}_{cel}] + E_{loc} E[\mathbb{T}_{loc}] \end{aligned} \tag{32}$$

5.3. Cellular versus local links

The performance of cooperation will depend on the slot rate and energy use per bit costs on the local and the cellular links. Therefore, we define the r_t as the ratio between cellular and local slot rate costs, and r_e as the ratio between the cellular and local energy cost.

$$r_t = \frac{t_{loc}}{t_{cel}} = \frac{R_{cel}}{R_{loc}} \;\; ; \;\; r_e = \frac{E_{b,cel}}{E_{b,loc}} \tag{33}$$

5.4. Gain regions

For the analysis with different erasure rates per stage, we define the throughput and energy gains of cloud cooperation against broadcast RLNC from (30) and (31) as shown in (35).

$$\begin{aligned} G_t &= \frac{E[\mathbb{T}_{cel}]}{\max(r_t E[\mathbb{T}_{cel}], E[\mathbb{T}_{loc}])} \\ G_e &= 1 - \frac{r_e \left(\frac{H}{N} \right) E[\mathbb{T}_{cel} + \mathbb{T}_{loc}]}{r_e E[\mathbb{T}_{loc}]} \end{aligned} \tag{34}$$

We define throughput gain as the ratio of the cloud cooperation and broadcast RLNC throughputs. The energy gain of cooperation over broadcast is defined as the saving in energy for the devices, because cooperation always save energy at the BS.

5.5. Optimal cloud size

All the studied scenarios can be regarded as the spectrum of cooperation, where broadcast is the case of no cooperation, single cloud cooperation the case of full cooperation and multiple clouds cooperation the in-between. Then, we define the optimal cloud size as the size that all the clouds should have in order to minimise the total transmission time. We consider this because we have observed that in the case of having the same erasure rate for all the links in the cellular stage and the same erasure rate for all the links in the local stage, employing the same cloud size for all the clouds, two main situations dominate either the cellular or the local transmission time. First, the cellular transmission time mostly depends on the smallest cloud, for example, the one with the least amount of devices. Second, the local transmission time depends on the remaining devices to be served, which is proportional to the biggest cloud. We verify this in the results section and then focus on the homogeneous case because it gives the best performance. For this case, there will be a trade-off for the number of transmissions in each stage. For the broadcast case, we simply consider that $N_{uc} = 1$ and $\mathbb{T}_{MCC,loc} = 0$. Thus, the optimal cloud size is defined as follows:

$$N^*_{uc} = \min_{N_{uc}} \mathbb{T}_{MCC} \tag{35}$$

5.6. Overhead

We calculate the performance of TC against RLNC by reviewing the optimal field choices that minimises an overhead-related cost function and compare them against the performance of both RLNC with $GF(2)$ and $GF(2^8)$ given that they represent opposite extremes.

We define the overhead for a field scheme s and transmission scenario t as

$$\mathbb{O}_{s,t} = (B + |\boldsymbol{v}|_{s,t})(\mathbb{T}_{s,t} - \mathbb{T}_{s_{min},t}) + |\boldsymbol{v}|_{s,t} \mathbb{T}_{s_{min},t} \text{ [bits]} \tag{36}$$

In (36), $\mathbb{O}_{s,t}$ is the overhead viewed as random variable depending on a given scheme and transmission scenario. $|\boldsymbol{v}|_{s,t}$ is the coding coefficients overhead for the given scheme and scenario. $\mathbb{T}_{s,t}$ is the (random) number of transmissions of the given scheme and scenario and $\mathbb{T}_{s_{min},t}$ is a

random variable for the minimum amount of transmissions that the scheme might take in the given scenario. A reasonable approximation for this variable is $\mathbb{T}_{GF(2^8),t}$. Given that we are evaluating the overhead, our choice for the cost function to obtain the optimal field scheme is the mean overhead. Then, the optimal field scheme for a given scenario is the one that minimises the following cost function (after rearranging terms):

$$\begin{aligned} \min_{\boldsymbol{q}} \quad & (B + |\boldsymbol{v}|_{\boldsymbol{q},t})E[\mathbb{T}_{\boldsymbol{q},t}] \\ \text{s.t.} \quad & \boldsymbol{q}_i = 2^{2^{k_i}},\ i \in [1, g],\ k_i \in \mathbb{Z}^+ \end{aligned} \tag{37}$$

In the nonlinear integer problem defined in (37), we have substituted the scheme subscript to highlight the dependence on the fields of the mean overhead minimisation because the optimal scheme is a particular choice of fields. For a given solution of (37), we evaluate its cost in (36) to review the performance of the given scheme.

6. NUMERICAL RESULTS

We use a set of parameters in the following ranges $1 \leqslant N \leqslant 50$, $g = \{64, 128\}$, $q = 2^8$ and $0 \leqslant \epsilon_{cel} = \epsilon_{loc} = \epsilon \leqslant 0.6$. The time slot duration is set to $t_{cel} = 0.5$ ms to conform to the LTE-A E-UTRA [29] and its set of D2D specifications. For the energy, we extracted the energy per bit cost from the energy model in [28] and use a packet size N_B of 500 B. For RLNC, in case of increasing the packet size (e.g. 1.5 KB) while keeping the total amount of data, the overhead contribution from the coding coefficients will be low because the amount of bits required to send the coding coefficients will be less than the required packet size, reducing the required signalling. For the case of a low packet size (e.g. 100 B), the overhead due to the coding coefficients per packet increases because it is comparable with or even higher than the packet size. Then, for very low packet sizes, most of the information sent is mainly signalling reducing the throughput. For the overhead of TC, we evaluate broadcast and single cloud cooperation with a set of parameters in the following ranges $N = \{1, 30, 50\}$, $g = \{16, 32, 64, 128\}$, $\epsilon_{cel} = \epsilon_{loc} = \epsilon = \{0.1, 0.3, 0.5\}$. We use a representative wireless network packet size of 1.6 KB ($B = 12\,800$ bits). For the optimal field scheme, we obtain the solutions that minimise the cost function in (37) by performing a search for the solutions in the feasible set of (37) and verifying which minimises the cost function. The considered field sizes for the feasible set were 2, 2^2, 2^4, 2^8, 2^{16} and 2^{32} as in [19], because current computer data types can easily represent these values. Following, we make the comparison in percentage value obtained as $E[\mathbb{O}_{s,t}]/gB \times 100\%$.

Figure 4 shows how the throughput varies depending on the ratio of the cellular and local data rate. The ratios are obtained by fixing the cellular data rate and varying the local data rate. When the local data rate is lower than the cellular rate, the cooperative schemes provide lower throughput than the broadcast scheme. Conversely, when the local data rate is higher than the cellular data rate, the cooperative schemes deliver a higher throughput than broadcast. The throughput is highest when the local links rate are twice as faster as the cellular ones. The number of heads controls how much gain can be obtained and where it occurs for a given ratio. When the number of heads decreases, the throughput also diminishes because there are fewer heads each with an independent chance of receiving the packet.

Figure 5 shows how the energy for the devices changes as the ratio between the cellular and local energy per bit changes. The energy cost in the cellular link is fixed and the cost on the local link is changed to obtain the different ratios; consequently, the energy per bit for broadcast is constant.

When the energy cost for the local links is higher than the cellular energy cost, the cooperation performs worse than broadcast. The extra consumption for cooperation comes from the transmissions in the local stage. Contrarily, when the cost of the local links is lower than the cost of

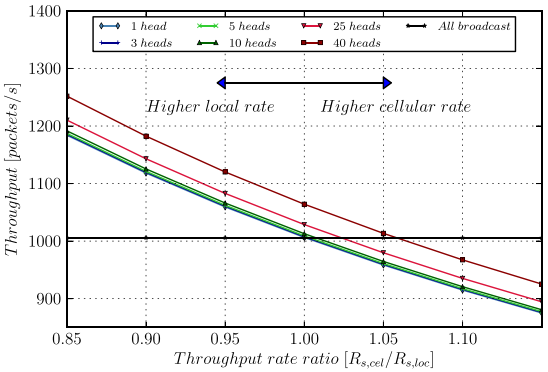

Figure 4. The throughput of broadcast and cooperation with different number of heads, for different ratios between the data rate on the cellular and local link. Used parameters: $g = 64$, $q = 2^8$, $\epsilon = 0.4$, $N = 50$.

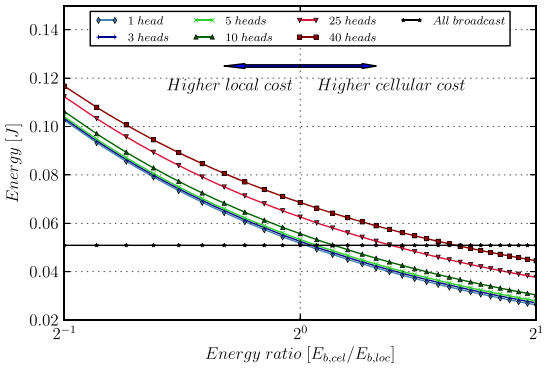

Figure 5. The energy per generation of broadcast and cooperation with different number of heads, for different ratios between the energy per bit on the cellular and local link. Used parameters: $g = 64$, $q = 2^8$, $\epsilon = 0.4$, $N = 50$.

DOI: 10.1002/ett

the cellular links, single cooperation uses less energy than broadcast. In these cooperation scenarios, the consumption is determined by the number of heads on the cellular stage.

For a cloud of a determined size, in the case of having the same erasure rate for all the links in the cellular stage, there is a trade-off between throughput and energy expenditure that depends on the number of heads. The higher number of heads, the higher the throughput. When a coded packet is broadcasted to the cloud in the cellular stage, having more heads cooperating with each other rapidly increases the probability that at least one of them obtains it, to later share this knowledge with all the devices. This in turn increments the probability of having all the packets inside the cloud in g transmissions, enhancing the throughput. However, this comes at the expense of higher energy consumption because more energy is spent when receiving the packets to the cloud. For a low amount of heads, the energy expenditure for the devices is low, but the same for the throughput given that more transmission is required because less devices are cooperating. At the end, it is a design decision because both benefits cannot be achieved at the same time.

Figure 6 shows the regions where cooperation provides a gain in terms of throughput for a wide range of erasure rates on the cellular and local links. The lines show where broadcast and cooperation perform the same, for $r_t = [0.5, 0.8, 1, 1.5, 2]$. In the region below each line, cooperation provides higher throughput than broadcast for that particular r_t. Above the line, broadcast performs better. For example, in the case of a fast local link $r_t = 0.5$, then cooperation provides a gain for almost all considered erasure rates, even in cases where the local erasure rate is much higher than the cellular.

Figure 7 shows the regions where cooperation provides a gain in terms of energy saving on the devices for various erasure rates on the cellular and local links. The lines show where broadcast and cooperation performs the same, for $r_e = [0.5, 0.75, 1, 1.5, 2]$. In the region below each line, cooperation provides a lower energy per bit than broadcast for that particular r_e. Above the line, broadcast performs better.

Figure 8 shows the results for two simulations. The first simulation shows the cellular transmission time for two different scenarios. In the first scenario, for the same losses in the cellular stage, $\epsilon_{cel} = 0.3$, we show the cellular transmission time for two clouds where the first cloud size is fixed to six devices and the second cloud size ranges from one to 20 devices. In the second scenario, for the same losses in the cellular stage, we show the transmission time for five clouds where all the cloud sizes are the same. We vary the size of all these clouds from one to 20 devices.

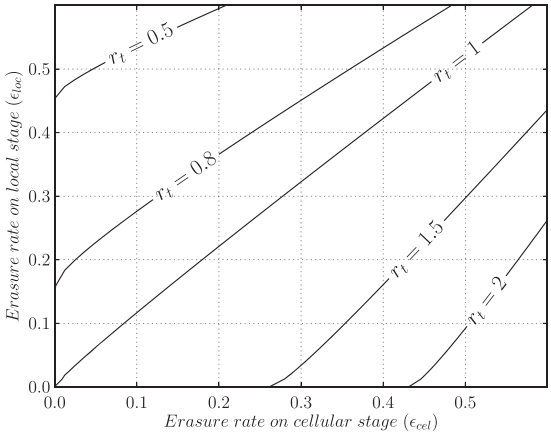

Figure 6. For different values of r_t, the lines indicate where cooperation and broadcast provide the same throughput for various erasure rates on the cellular and local links. Below each line, cooperation performs better for the respective r_t. Used parameters: $g = 128$, $q = 2^8$, $H = 40$, $N = 50$.

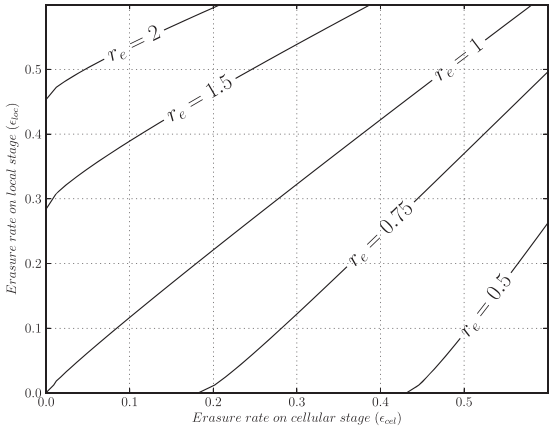

Figure 7. For different values of r_e, the lines indicate where cooperation and broadcast provide the same energy per bit for various erasure rates on the cellular and local links. Below each line, cooperation performs better for the respective r_e. Used parameters: $g = 128$, $q = 2^8$, $H = 40$, $N = 50$.

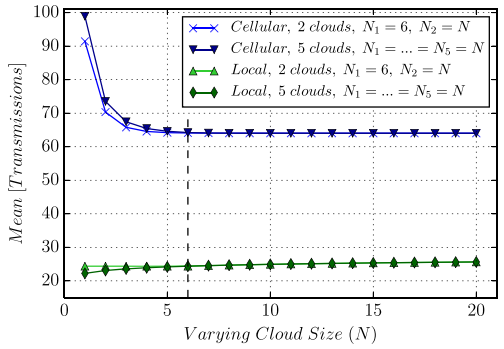

Figure 8. For the cellular transmission time, the smallest cloud dominates the transmissions below the homogeneous size (dashed line). Above it, it remains mostly constant. For the local transmission time, it remains constant below the homogeneous size (dashed line). Above it, the biggest cloud starts to slowly dominate the transmissions. Used parameters: $g = 64$, $q = 2^8$, $\epsilon_{cel} = 0.3$, $\epsilon_{cel} = 0.1$, $H = N$, N varies.

For the first scenario, we observe that as the number of devices in the second clouds is less than six (dashed line), then transmission time in the cellular stage increases given that this cloud requires more transmissions than the first cloud. For the second scenario, as we increase the number of devices in the five clouds, the error between one varying cloud and five varying clouds becomes very small.

The second simulation shows the trends for the local transmission time similarly in two scenarios. In the first scenario, assuming equal losses in the local stage, $\epsilon_{loc} = 0.1$, we present the local transmission time for two clouds keeping fixed the size of the first one to six devices and varying the size of the second from one to 20 devices. In the second scenario, for equal losses in the local stage, we present the local transmission time where all the clouds have the same size, and we vary them from one to 20 devices. Here, for the first scenario, we notice that the local transmission time is higher when second cloud size is bigger than the first one. The reason being that the second cloud becomes the biggest one and dominates the local transmission time. Similarly, for the second scenario, we observe that the local transmission time matches for both cases after six devices (dashed line).

At the end, we see that the homogeneous is the best case that we could obtain. In any other case, one of the following two situations occurs: (i) the cellular transmission time is high, while the local transmission time is constant, or (ii) the cellular transmission time remains constant, while local transmission time is high. The homogeneous case is simply the boundary between the previous two.

Figure 9 shows the trade-off for the number of users per cloud for different given erasure rate in the cellular and local stages. We clearly observe that there is a cloud size N_{uc} for which the total number of transmissions $\mathbb{T}_{MCC}$ is minimum, thus minimising the energy consumption and maximising the throughput.

We study the overhead performance for the three schemes for both scenarios to compare the optimal scheme performance.

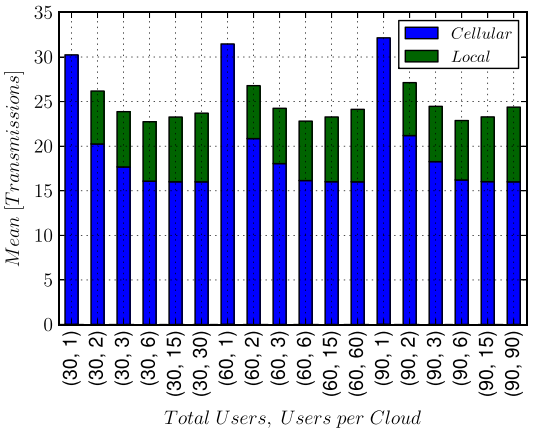

Figure 9. Optimal cloud size for $g = 16$, $q = 2^8$, $\epsilon_{cel} = 0.3$ and $\epsilon_{loc} = 0.1$.

6.1. Optimal telescopic codes configuration and performance for broadcast

Figure 10(a) first shows the optimal scheme obtained from solving (37). Second, Figure 10(b) shows the corresponding optimal scheme overhead against the overhead from the other two code schemes. Both results are for 30% losses in all the links of the remote stage. Both the optimal field scheme and overhead are presented versus the combinations of users, N, and generation sizes, g. Each bar in Figure 10(a) indicates the amount of coding coefficients for the given fields as percentages in the generation. For all shown combinations in Figure 10(a), as g increases for a fixed amount of users, most of the coefficients are drawn from $GF(2)$ with a diminishing percentage being chosen from other fields. Nevertheless, for a fixed generation size and increasing number of users, only for low values of g it can be observed a tendency to use more coding coefficients in high fields. Figure 10(b) exhibits the overhead mean of the three schemes. For all the cases, we see that the optimal

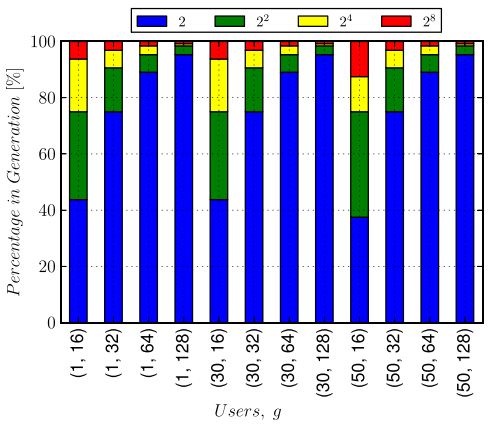

(a) Optimal field scheme, q^*

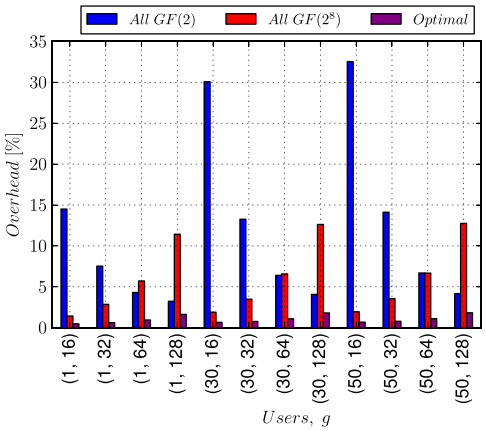

(b) Overhead mean (%)

Figure 10. Schemes performance for broadcast. $\epsilon = 0.3$.

DOI: 10.1002/ett

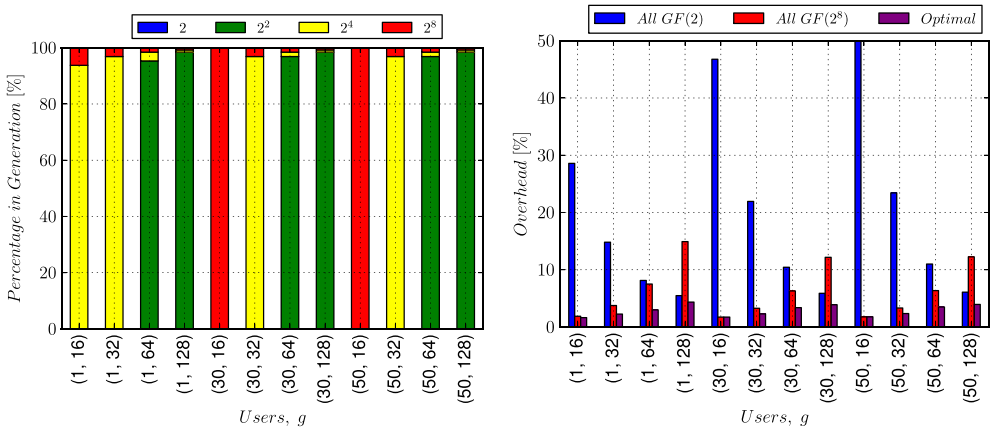

(a) Optimal field scheme, q^*

(b) Overhead mean (%)

Figure 11. Schemes performance for cloud cooperation. $\epsilon = 0.3$.

Table I. Scenarios and schemes comparison.

Transmission scenario	Code scheme	Overhead	Transmission time			*Energy	*Throughput
			Cellular	Local	Total		
Broadcast	RLNC	Med	High	None	High	Med	Low
	Telescopic	Low	High	None	High	Low	Low
Single cloud cooperation	RLNC	Med	Low	Med	Med	High	Med
	Telescopic	Low	Low	Med	Med	High	Med
Multiple clouds cooperation	RLNC	Med	Low	Low	Low	Med	High
	Telescopic	Low	Low	Low	Low	Low	High

$\epsilon_{cel} = 0.3, \epsilon_{loc} = 0.1,\ N = 60,\ H = N,\ r_e \leqslant 1,\ r_t \geqslant 1$.
RLNC, random linear network coding.

field scheme outperforms both $GF(2)$ and $GF(2^8)$ achieving a less than 2% total overhead in most of the cases. For $g \leqslant 32$, increasing the number of receivers greatly affects the total overhead, almost doubling it in the case of $g = 16$. Although, for $g \geqslant 64$, the overhead is less sensitive to the number or receivers.

6.2. Optimal telescopic codes configuration and performance for single cloud cooperation

Correspondingly, Figure 11 exhibits the performance for cloud cooperation. Figure 11(a) presents the optimal scheme obtained from solving (37) for cloud cooperation and 30% losses for both the remote and local links. In this case, for increasing g and fixed users amount, more than 90% of the coding coefficients belong to a single field. For $g \leqslant 32$, the scheme distribution goes mostly to either $GF(2^4)$ or $GF(2^8)$. For $g \geqslant 64$, most of the coefficients are chosen from $GF(2^2)$. For a fixed generation size and varying amount of users, the coding coefficients distribution appreciably changes for $g = 16$ and slightly for $g = 64$. Figure 11(b) displays the overhead mean; the optimal field scheme provides a lower mean overhead than both $GF(2)$ and $GF(2^8)$, except for the cases of 30 and 50 receivers with 16 packets as generation size, where the optimal scheme and subsequently mean overhead are the same as $GF(2^8)$. Still, for all the cases, total overhead mean does not exceed 2.5% with some cases being approximately less than 1%.

Finally, in Table I, we present a solution comparison to show our major results. We consider a packet erasure rate of 30% for the cellular links and 10% for the local links. Similarly, we consider a large fixed amount users, $N = 60$, with all of them being heads. Also, the energy cost in the cellular stage is equal or higher as the energy cost in the local stage ($r_e \leqslant 1$). Similarly, we consider that duration of a time slot in the cellular stage is the same as in the local stage ($r_t \geqslant 1$). Under this scenario, the multiple clouds cooperation approach provides the best performance in terms of throughput. Thus, we expect the highest gains from cooperation and coding in this regime.

7. CONCLUSIONS

In this work, we presented an in-depth study of the specific operating regions where cooperation provides gains in throughput and energy over coded broadcasting techniques. Our numerical results showed that gains can be achieved even if the long-range and short-range

technologies transmit at comparable data rates or there are few differences in the erasure rates in each stage. More importantly, we showed that cooperation can provide several fold gains broadcast as long as the short-range link is at least twice as fast as the long-range one. Finally, our results showed that a moderate number of heads (e.g. three or more) per cooperative cluster is enough to yield the high throughput gains while maintaining a low energy consumption at the receivers. Also, for multiple clouds cooperation, we observed that the cloud size should be around six nodes in most of the cases.

We also proposed the use of TC for network-coded cooperative to reduce the total system overhead. We review the performance of TC against classical RLNC systems using either $GF(2)$ or $GF(2^8)$ with two common multicast scenarios: broadcast and single cloud cooperation. For a broadcast scenario, we observed that the optimal field scheme always outperforms both traditional RLNC schemes where in some cases total overhead is less than 0.5%. For single cloud cooperation, the total overhead was less than approximately 3% in all the cases. In a single cloud cooperation scenario, the penalty for including coefficients from low fields becomes significant because of the presence of the hops. However, this becomes less critical as the generation size increases.

Future work shall focus on protocol design for cooperative schemes in highly dense scenarios as well as implementation and evaluation of the most promising schemes in Aalborg University's Raspberry Pi testbed [30]. Regarding optimal overhead codes, future work in this area should consider the inclusion of other scenarios such as multiple clouds cooperation and multihops.

APPENDIX

Proof of Lemma 4.1

Let $\mathbb{T}_{TC,i}$ be a random variable for the number of transmissions needed to receive an l.i. coded packet in a stage of the Markov Chain for TC in Figure 3. This is a geometric distribution[†] with success probability given by $p_i = 1 - \boldsymbol{q}_i{}^{-g+(i-1)}, i \in [1, g]$. In general, $\boldsymbol{q}_i = 2^{2^{k_i}}, k_i \in \mathbb{Z}^+$. Later, the distribution for TC is given as follows:

$$\mathbb{T}_{TC} = \sum_{i=1}^{g} \mathbb{T}_{TC,i} \tag{A.1}$$

A direct computation of (A.1) is analytically intractable due to the requirement of computing $g-1$ discrete convolutions. Nevertheless, in the pgf domain, this operation turns into a product making the analysis fairly easier.

First, let us define the pgf of a discrete random variable $\mathbb{T}$ from its pmf as $G_{\mathbb{T}}(z) = E[z^{\mathbb{T}}] = \sum_{t=-\infty}^{\infty} \Pr[\mathbb{T} = t]z^t = \sum_{t=-\infty}^{\infty} f_{\mathbb{T}}(t)z^t$. Second, the bilateral Z-transform of the pmf as $F(z) = \mathcal{Z}\{\Pr[\mathbb{T} = t]\} = \sum_{t=-\infty}^{\infty} \Pr[\mathbb{T} = t] = \sum_{t=-\infty}^{\infty} f_{\mathbb{T}}(t)z^{-t}$. Doing little algebra with the previous two definitions, it can be seen that $F(z) = G_{\mathbb{T}}(z^{-1})$. Thus, the Z-transform of (A.1) becomes

$$F_{\mathbb{T}_{TC}}(z) = \prod_{i=1}^{g} G_{\mathbb{T}_{TC,i}}(z^{-1}) \tag{A.2}$$

Calculating the pgf of $\mathbb{T}_{TC,i}$ with the previous definitions and inserting in (A.2), we obtain the following:

$$\begin{aligned} F_{\mathbb{T}_{TC}}(z) &= G_{\mathbb{T}_{TC}}(z^{-1}) \\ &= \prod_{i=1}^{g} \frac{p_i z^{-1}}{1-(1-p_i)z^{-1}} \ , \ |z| > \max(1-p_i) \end{aligned} \tag{A.3}$$

In (A.3), we notice $\prod_{i=1}^{g} p_i$ is simply the probability of decoding in exactly g transmissions, $\Pr[\mathbb{T}_{TC} = g]$, which we relabel as P_g. Also, $\gamma_i = 1 - p_i$ is probability of obtaining an l.d. in stage i. Including this (A.3), we obtain

$$F_{\mathbb{T}_{TC}}(z) = P_g z^{-g} \prod_{i=1}^{g} \frac{1}{1-\gamma_i z^{-1}} \ , \ |z| > \max(\gamma_i) \tag{A.4}$$

From (A.4), we analytically observe the following: First, as expected, the pmf will be a right handed, causal and stable sequence from the signal processing perspective. The reason being that the pmf Z-transform Region of Convergence includes $|z| = \infty$ and $|z| = 1$ because $\max(\gamma_i) < 1$ always. Also, the pmf sequence will begin at g because of the delay term z^{-g}, which makes reference to the fact that g transmissions are required to receive g l.i. packets.

At this point, we make the following observation: Depending on the field distribution considered, at least some of the l.d. probabilities may be equivalent to each other. Thus, in general, the Z-transform of the TC, (A.4), may have repeated roots in its pgf. Therefore, let us consider that we have γ_l, $l \in [1, L]$ distinct l.d. probabilities in the Markov Chain in Figure 3, each repeated m_l times with $\sum_{l=1}^{L} m_l = g$. Then, (A.4) becomes (A.5):

$$F_{\mathbb{T}_{TC}}(z) = P_g z^{-g} \prod_{l=1}^{L} \frac{1}{(1-\gamma_l z^{-1})^{m_l}} \ , \ |z| > \max(\gamma_l) \tag{A.5}$$

Afterwards, we perform a partial fraction expansion on the product term in (A.5), which is rational, which turns it into

$$F_{\mathbb{T}_{TC}}(z) = P_g z^{-g} \sum_{l=1}^{L} \sum_{n=1}^{m_l} \frac{a_{l,n}}{(1-\gamma_l z^{-1})^n} \ , \ |z| > \gamma_{l_{max}} \tag{A.6}$$

In (A.6), we have splitted the product as a sum of the contributions of each of its poles of the Z-transform in (A.6). Here, RLNC appears as a special subcase due to the

[†]We use the definition of the geometric distribution that accounts for the random number $\mathbb{T}$ of Bernoulli trials of success probability p required to obtain the first success. Later, if $\mathbb{T} \sim Geom(p) \implies \Pr[\mathbb{T} = t] = (1-p)^{t-1}p \ , \ t \in [1, \infty)$

linear dependence probabilities being unique in that case. Hence, we can obtain the pmf for RLNC as a subcase of the for TC.

From (A.6), the $a_{l,n}$ coefficients $a_{l,n}$, $l \in [1, L]$, $n \in [1, m_l]$ are the residues of the complex function $\left[\prod_{m=1}^{L}(1-\gamma_m z^{-m_l})\right]^{-1}$ at the poles $z = \gamma_l$, $l \in [1, L]$. These residues are calculated using the expression:

$$a_{l,n} = \frac{\lim_{z\to\gamma_l} \frac{d^{m_l-n}}{d(z^{-1})^{m_l-n}} \left(\frac{G_{\mathbb{T}_{TC}}(z^{-1})(1-\gamma_l z^{-1})^{m_l}}{P_g z^{-g}}\right)}{(m_l-n)!(-\gamma_l)^{m_l-n}} \quad \text{(A.7)}$$

Performing this evaluation and doing inverse Z-transform algebra, the one obtains (6), which concludes the proof.

Proof of Corollary 4.1.1 The proof comes by letting $\boldsymbol{q}_i = q \ \forall i \in [1, g]$, which gives different unique l.d. probabilities in the Markov Chain, which in turns gives all simple poles (A.4). This makes quite easy to evaluate the residues as $a_i = \lim_{z\to\gamma_i}\left[\prod_{m=1}^{g}(1-\gamma_m z^{-1})\right]^{-1} \times \left[(1-\gamma_i z^{-1})\right]$ and noting that the relationship $\gamma_m \gamma_i^{-1} = q^{m-i}$ between the l.d. probabilities giving the result in (8), and this concludes the proof.

Proof of Lemma 4.2 For the probability of the maximum number of transmissions of the worst receiver to be less than or equal to t transmissions, then necessarily all other receivers must also have this (or in general less) transmissions than the worst receiver.

Therefore, under the packet erasures independence assumption, we can compute the cumulative density function (CDF) for broadcast with TC, as $F_{\mathbb{T}_B}(t) = \Pr[\mathbb{T}_B \leqslant t] = \prod_{j=1}^{N} \Pr[\mathbb{T}_{U_j} \leqslant t]$ with $\Pr[\mathbb{T}_{U_j} \leqslant t]$ being the CDF obtained from the pmf in (10) with the resulting CDF in (A.8).

$$F_{\mathbb{T}_B}(t; N, g, \boldsymbol{q}, \epsilon_1, \ldots, \epsilon_N) = \prod_{j=1}^{N}\left(\sum_{k=g}^{t}\sum_{i=g}^{k}\binom{k-1}{i-1}(1-\epsilon_j)^i \epsilon_j^{k-i} f_{\mathbb{T}_{TC}}(i; g, \boldsymbol{q})\right) \quad \text{(A.8)}$$

Finally, to obtain the pmf for broadcast, we simply compute $f_{\mathbb{T}_B}(t) = F_{\mathbb{T}_B}(t) - F_{\mathbb{T}_B}(t-1)$, which gives (11).

Proof of Lemma 4.3 In the cellular stage, each coded packet is acknowledged as received if at least one head obtains it, regardless if it is l.i. or not. This event occurs with probability $1 - \prod_{j=1}^{H} \epsilon_j$ because all links need to fail for a packet to not be received. Therefore, the distribution of the number of transmissions to obtain a coded packet is $Geom(1 - \prod_{j=1}^{H} \epsilon_j)$. Because we need to account for g packets, the distribution for receiving all the packets without considering the coding scheme is $NB(g, 1 - \prod_{j=1}^{H} \epsilon_j)$ given that it is the sum of g geometric distributions. Later, we couple the resulting pmf with the coding scheme one by following the same procedure as in the proof of Lemma 4.1 to obtain (10). Doing the calculations, we obtain (13).

In the local stage, the heads take turns to broadcast their content between all devices in the cloud. Given that we have assumed coordination among the heads, any temporal transmitting head behaves as a source broadcasting recoded packets. Then, the pmf for this stage is a particular case of (12).

At this point, we differentiate two cases: not all heads and all heads. For the former, we make the approximation that the non-heads will become the dominant factor in the broadcast pmf, given that they have no collected packets from the previous stage. In case of the latter, there is no dominant set of devices with a particular number of packets. So, in general, we need to exclude from the total amount of devices, N, the devices that may have finished before (although depending on the conditions this number might be very low) and account that some devices have some packets already.

To obtain an average number of devices that may have finished in the cellular stage for the all heads case, N_f, we approximate it as the mean for the random number of devices that have g l.i. packets after exactly g transmissions have occurred. We round down this to provide an integer result, so $N_f = \lfloor E[\mathbb{N}_f] \rfloor$. Assuming that g transmissions occur in the cellular stage is reasonable because the mean of the distribution in (13) is $g/(1 - \prod_{j=1}^{N} \epsilon_j)$. This mean tends to g rapidly for practical values of the ϵ_j and N.

To calculate the distribution of the devices that have finished, $\mathbb{N}_f$, we notice that each device meeting the previous condition can be regarded as a Bernoulli trial with success probability $P_g(1-\epsilon_j)^g$ because all packets must be received and l.i. for each device independently. So, we consider $\mathbb{N}_f = \sum_{j=1}^{N} Bernoulli(P_g(1-\epsilon_j)^g)$ and taking the mean to this expression gives $E[\mathbb{N}_f] = \sum_{j=1}^{N} E[Bernoulli(P_g(1-\epsilon_j)^g)] = P_g \sum_{j=1}^{N}(1-\epsilon_j)^g$. Later, $N_f = \lfloor E[\mathbb{N}_f] \rfloor = \lfloor P_g \sum_{j=1}^{N}(1-\epsilon_j)^g \rfloor$ from which we obtain $N_{loc} = N - N_f$, which gives (15).

To obtain how many packets we need to transmit in the local stage, we calculate how many packets does each device j, $j \in [1, N]$ has on average after g transmission have occurred rounded down, $\lfloor E[\mathbb{G}_j] \rfloor$. Then, we will transmit as many coded packets as required to ensure that the device that has the less number of packets from the cellular stage acquires the whole generation, for example, $g_{loc} = \max_j(g - \lfloor E[\mathbb{G}_j] \rfloor)$.

For the j-th device, in g transmissions, it will have received $\mathbb{G}_j$ l.i. packets. The i-th transmission with $i \in [1, g]$ can be regarded as a Bernoulli trial that has success probability $p_i(1-\epsilon_j)$. Thus, $\mathbb{G}_j = \sum_{i=1}^{g} Bernoulli(p_i(1-\epsilon_j))$ for which its mean is $(1-\epsilon_j)\sum_{i=1}^{g} p_i$. Then, doing the remaining algebra, we obtain (16), and this concludes the proof.

Proof of Lemma 4.4 This proof is similar as the preceding one, but some differences occur. First, instead of broadcasting to a single cloud in the cellular stage, we broadcast to $1 < n < C$ clouds, so the number of transmissions will be upper bounded by the worst cloud, hence the computation as described in (21). Second, in the local stage, we calculate the new parameters for

evaluating the distributions in each cloud depending on the cloud being considered in general because the parameters depend on the erasure rates of cellular stage. Nevertheless, the results from the proof of Lemma 4.3 still hold.

ACKNOWLEDGEMENTS

This research has been partially financed by the CROSSFIRE MITN Marie Curie project (317126) from the European Commission FP7 framework and the Green Mobile Cloud project (grant no. DFF - 0602- 01372B) granted by the Danish Council for Independent Research. Also, we would like to thank former Vodafone CTO, Eng. Hartmut Kremling, for providing data consumption trends in current well-deployed mobile networks.

REFERENCES

1. Kremling H. *Innovation at Vodafone: 5G and the Internet of Things*, Vodafone Annual Meeting: Dresden, Germany, 2015.
2. Fitzek FHP, Katz MD. *Cooperation in Wireless Networks: Principles and Applications—Real Egoistic Behaviour is to Cooperate!* Springer: Dordrecht, The Netherlands, 2006. https://books.google.dk/books?id=iSWmPZS_yvkC [available on 15 December 2015].
3. Lin X, Andrews JG, Ghosh A. A comprehensive framework for device-to-device communications in cellular networks. *arXiv preprint ArXiv:1305.4219* 2013.
4. 3GPP. Feasibility study for proximity services (prose). *TR 22.803. Release 12*, 3rd generation partnership project; technical specification group: system aspects (SA), 2012. http://www.3gpp.org/ftp/Specs/html-info/22803.htm [available on 15 December 2015].
5. Fitzek FHP, Katz MD. *Mobile Clouds: Exploiting Distributed Resources in Wireless, Mobile and Social Networks*. Wiley: Hoboken, New Jersey, USA, 2013. https://books.google.dk/books?id=s2lXAgAAQBAJ [available on 15 December 2015].
6. Heide J, Fitzek FH, Pedersen MV, Katz M. Green mobile clouds: network coding and user cooperation for improved energy efficiency. In *Cloud Networking (Cloudnet), 2012 IEEE 1St International Conference on*, Paris, France, 2012, IEEE; 111–118.
7. Ahlswede R, Cai N, Li S-YR, Yeung RW. Network information flow. *Information Theory, IEEE Transactions on* 2000; **46**(4): 1204–1216.
8. Ho T, Médard M, Koetter R, Karger DR, Effros M, Shi J, Leong B. A random linear network coding approach to multicast. *Information Theory, IEEE Transactions on* 2006; **52**(10): 4413–4430.
9. Eryilmaz A, Ozdaglar A, Médard M, Ahmed E. On the delay and throughput gains of coding in unreliable networks. *Information Theory, IEEE Transactions on* 2008; **54**(12): 5511–5524.
10. Khamfroush H, Lucani DE, Barros J. Minimizing the completion time of a wireless cooperative network using network coding. In *Personal Indoor and Mobile Radio Communications (PIMRC), 2013 IEEE 24th International Symposium on*, London, UK, 2013, IEEE; 2016–2020.
11. Khamfroush H, Lucani DE, Pahlevani P, Barros J. On optimal policies for network coded cooperation: theory and implementation. *IEEE Journal on Selected Areas in Communications* 2015; **33**(2): 199–212.
12. Heide J, Pedersen MV, Fitzek FH, Larsen T. Network coding for mobile devices-systematic binary random rateless codes. In *Communications Workshops, 2009. ICC Workshops 2009. IEEE International Conference on*, Dresden, Germany, 2009, IEEE; 1–6.
13. Chou PA, Wu Y, Jain K. Practical network coding, 2003.
14. Trullols-Cruces O, Barcelo-Ordinas JM, Fiore M. Exact decoding probability under random linear network coding. *Communications Letters, IEEE* 2011; **15** (1): 67–69.
15. Zhao X. Notes on exact decoding probability under random linear network coding. *Communications Letters, IEEE* 2012; **16**(5): 720–721.
16. Heide J, Pedersen MV, Fitzek FH, Médard M. On code parameters and coding vector representation for practical RLNC. In *Communications (ICC), 2011 IEEE International Conference on*, Kyoto, Japan, 2011, IEEE; 1–5.
17. Paramanathan A, Pedersen MV, Lucani DE, Fitzek FH, Katz M. Lean and mean: network coding for commercial devices. *Wireless Communications, IEEE* 2013; **20** (5): 54–61.
18. Li X, Mow WH, Tsang FL. Singularity probability analysis for sparse random linear network coding. In *Communications (ICC), 2011 IEEE International Conference on*, Kyoto, Japan, 2011, IEEE; 1–5.
19. Heide J, Lucani D. Composite extension finite fields for low overhead network coding: telescopic codes. In *IEEE International Conference on Communications (ICC)*, London, UK, 2015.
20. Chiti F, Fantacci R, Schoen F, Tassi A. Optimized random network coding for reliable multicast communications. *Communications Letters, IEEE* 2013; **17** (8): 1624–1627.
21. Tassi A, Chatzigeorgiou I, Vukobratovic D. Resource-allocation frameworks for network-coded layered multimedia multicast services. *Selected Areas in Communications, IEEE Journal on* 2015; **33**(2): 141–155.
22. Militano L, Condoluci M, Araniti G, Molinaro A, Iera A, Fitzek FH. Wi-Fi cooperation or D2D-based multicast

content distribution in LTE-A: a comparative analysis. In *Communications Workshops (ICC), 2014 IEEE International Conference on*, Sydney, Australia, 2014, IEEE; 296–301.

23. Militano L, Condoluci M, Araniti G, Molinaro A, Iera A. When D2D communication improves group oriented services in beyond 4G networks. *Wireless Networks* 2014; **21**(4): 1363–1377.
24. Condoluci M, Militano L, Araniti G, Molinaro A, Iera A. Multicasting in LTE-A networks enhanced by device-to-device communications. In *Globecom Workshops (GC Wkshps), 2013 IEEE*, Atlanta, Georgia, USA, 2013, IEEE; 567–572.
25. Militano L, Condoluci M, Araniti G, Molinaro A, Iera A, Muntean M. Single frequency-based device-to-device-enhanced video delivery for evolved multimedia broadcast and multicast services. *IEEE Transactions on Broadcasting* 2015; **61**(2): 263–278.
26. Fragouli C, Le Boudec JY, Widmer J. Network coding: an instant primer. *ACM SIGCOMM Computer Communication Review* 2006; **36**(1): 63–68.
27. Lucani DE, Médard M, Stojanovic M. Random linear network coding for time division duplexing: field size considerations. In *Global Telecommunications Conference, 2009. GLOBECOM 2009. IEEE*, Honolulu, Hawaii, USA, 2009, IEEE; 1–6.
28. Lauridsen M, Noël L, Sørensen TB, Mogensen P. An empirical LTE smartphone power model with a view to energy efficiency evolution. *Intel Technology Journal* 2014; **18**(1): 172–193.
29. 3GPP. Requirements for further advancements for e-utra (lte-advanced). *TR 36.913. Release 8*, 3rd generation partnership project; technical specification group: radio access plenary (RAP), 2009. http://www.3gpp.org/ftp/Specs/html-info/36913.htm [available on 15 December 2015].
30. Paramanathan A, Pahlevani P, Thorsteinsson S, Hundebøll M, Lucani D, Fitzek F. Sharing the pi: testbed description and performance evaluation of network coding on the raspberry pi. In *2014 IEEE 79th Vehicular Technology Conference*, Seoul, South Korea, 2014; 1–5.